Journal of the Serbian Chemical Society
JSCS-info@shd.org.rs • www.shd.org.rs/JSCS
J. Serb. Chem. Soc. *85* (9) 1223–1235 (2020)
JSCS–5370
UDC 546.46'62–36.05:577.11:615.276
Original scientific paper

Fabrication of bionanocomposite based on LDH using biopolymer of gum arabic and chitosan-coating for sustained drug-release

MILAD ABNIKI, ALI MOGHIMI* and FARIBORZ AZIZINEJAD

Department of Chemistry, Varamin-Pishva Branch, Islamic Azad University, Varamin, Iran

(Received 11 October, revised 12 December 2019, accepted 14 January 2020)

Abstract: The study proposed a new formulation to the sustained delivery of mefenamate anions intercalated into Mg–Al layered double hydroxide (LDH) for oral administration. Different experimental conditions were evaluated to incorporate the mefenamic acid (MEF) and gum arabic (GUM) into LDH structure. The LDH–MEF and LDH–MEF/GUM were covered with chitosan (CHIT). In another experiment, LDH–Cl was used to adsorb mefenamate anions and evaluate the mechanism. The products of LDH were characterized by using different techniques such as FESEM (field emission scanning electron microscopy), XRD (X-ray diffraction), FTIR (Fourier transform infrared) spectroscopy and TGA (thermogravimetric analysis). The X-ray diffraction patterns and FTIR analyses confirmed that the MEF and GUM were successfully intercalated into the interlayer space of LDH. TG analysis verified that the thermal stability of intercalated MEF in the form of bionanocomposite (LDH–MEF/GUM/CHIT) was enhanced. Finally, In vitro drug release experiments of bionanocomposite at a pH of 1.2 (acidic medium) and a pH of 7.4 (phosphate buffer medium) showed sustained release profiles with mefenamate anions as an anti-inflammatory model drug.

Keywords: hybrid material; layered double hydroxide; anti-inflammatory drug; intercalation compounds; controlled release.

INTRODUCTION

In recent years, the development of efficient, biocompatible and cost-effective drug carriers has been one of the major challenges in the field of drug delivery. Furthermore, more research on drug delivery systems (DDS) intends to use more efficient nanomaterials as barriers to adjust the speed of release and to maintain the desired dose.[1–3] In this sense, the improvement of controlled DDS is extremely dependent on the selection of an appropriate carrier able to control the release of pharmaceutical agents.[4,5] In the past years, novel controlled DDS has

* Corresponding author. E-mail: alimoghimi@iauvaramin.ac.ir
https://doi.org/10.2298/JSC191011004A

Available on line at www.shd.org.rs/JSCS/
(CC) 2020 SCS.

been developed in bionanocomposites and also novel inorganic materials. Bionanocomposites are hybrids of organic–inorganic materials resulting from the assembly of biopolymers and inorganic nanoparticles. Due to their bio-characteristics, and thermal and chemical properties, they have been used as carriers for a wide range of diagnostic and therapeutic compounds, such as drugs, DNA, biomolecules and proteins.[6–9] Given the easy synthesis, cost-affectivity, biocompatibility, low toxicity, and biodegradability of LDHs, they are much applied in the fabrication of bionanocomposites for various applications, especially in the biomedical field.[10] The LDHs are a category of inorganic ionic compounds with the general formula of $[M(II)_{I-x}M(III)_x(OH)_2]^{+x}(A^{-n})_{x/n}\cdot mH_2O$, where M(II) and M(III) denote bivalent and trivalent metals, and A is a guest anion in the LDH interlayer. LDHs are a class of natural minerals with high anion exchange capability that could increase the chemical and thermal stability of intercalated species.[11] LDHs are more prominent than other mineral materials because of their good performance in drugs release and they have also been identified as been suitable for hosting anti-inflammatory drugs. Research of Silion *et al*. indicated that an LDH hybrid containing a non-steroidal anti-inflammatory drug (NSAIDs) increased the durability of the drug in the stomach, resulting in a long-term effect upon oral ingestion.[12]

The structural properties of LDH hybrids can be improved by using natural polymers, such as polysaccharides. For example, a recent study reported that a composite of chitosan and an LDH–drug hybrid increases the bioavailability and adsorption capacity of the drug and also reduces the release rate of the drug.[13] In addition, studies showed that special properties could be achieved by a polymer coating on the surface of LDH. The advantages of polymer coating on the surface of a LDH included improvement of the physical and chemical properties of the LDH hybrid, change in the solubility of the LDH hybrid in lipid or aqueous environment, increase in the thermal stability of the LDH and slowing of the release time.[14]

In this research, mefenamic acid was selected as an anti-inflammatory model drug to be intercalated within an LDH matrix. The amount of oral administration of MEF is mainly associated with its biopharmaceutical properties. Due to the poor solubility of MEF, a high dose of MEF is required for a therapeutic effect, thereby increasing the side effects of the drug. Hence, the co-intercalation of GUM biopolymer and MEF into LDH was investigated in order to improve the loading and release of MEF. The focus of this study was placed on the co-intercalation method, high drug-loading, structural, as well as thermal and sustained-release properties of a bionanocomposite. The purpose of the current study was the design and evaluation of a new formulation for the sustained delivery of a non-steroidal anti-inflammatory drug intercalated into LDH.

(CC) 2020 SCS.

EXPERIMENTAL

Materials

Magnesium oxide (MgO, 99 % of purity), aluminium chloride hexahydrate ($AlCl_3 \cdot 6H_2O$, 98.5 % of purity) and gum arabic were obtained from Merck (Darmstadt, Germany). Mefenamic acid (98 % purity) and chitosan (medium molecular weight) were provided by Sigma–Aldrich. A stock solution (500 mg L^{-1}) of the drug was prepared by dissolving the appropriate amount of MEF in ethanol and deionized water with a ratio (1:10). Acetate and phosphate buffers (0.01 M) were prepared to adjust the pH of the solutions. All other chemical agents were of analytical grade and used without further purification.

Instruments

Infrared spectra of the synthesized samples were recorded on a Perkin Elmer spectrometer FT-IR RX1. A Shimadzu spectrometer UV–Visible 1601PC was employed to evaluate the loading and release of MEF. The structure and the crystal size of the samples were determined by XRD analysis (Philips, PW1730). The surface morphology and particle size of bionanocomposite were characterized using a field emission scanning electron microscopy (Tescan, Mira III). Energy dispersive spectrum (EDS) analysis on field emission scanning electron microscopy (Tescan, Mira III with SMAX detector) was employed for a survey of the elemental composition of the bionanocomposite. The thermal stability of the samples was investigated by thermal gravimetric analysis (Toledo, sdt851e). The pH measurements were realized using a pH meter (Sense Line, F410T). The suspended samples were separated by centrifugation (Hettich, Universal 320). The prepared samples were dried in a vacuum oven (Shimazu, Unb 400). An ultrasonic apparatus (CT chromtech, Uc-5150b) was used for sonication.

Synthesis

Synthesis of layered double hydroxide (LDH–Cl). The synthesis of LDH–Cl was performed by the co-precipitation method described by Chitrakar *et al.*[15] MgO (0.02 mol) was added to 100 mL of a solution containing 0.06 mol of $AlCl_3$, and the mixture stirred at 30 °C for 2 days. The solid product was obtained by centrifugation, washed with distilled water, and dried at 25 °C.

Preparation of LDH–MEF hybrid. The LDH–Cl (0.2 g) synthesized in the previous step was placed in an ultrasonic apparatus for 30 min and then added to 50 mL of MEF solution (25 mL of the stock solution diluted to 50 mL with deionized water). The pH of the mixture was adjusted to 10 with 0.2 mol L^{-1} sodium hydroxide solution,[16] and stirred for 24 h. The product was separated by centrifugation, washed thoroughly with deionized water and dried in a vacuum oven at 25 °C for 48 h.

Preparation of LDH–MEF/CHIT. A homogeneous solution containing 0.2 g of chitosan was prepared in 25 mL of acetic acid (1 vol. %). Thereafter, 0.2 g of LDH–MEF was dispersed into the homogeneous chitosan solution and then the pH adjusted to 6 by the controlled addition of NaOH under magnetic stirring for 2 h. Then, the pH of the mixture was adjusted to 7 and the product was separated by centrifugation and washed several times with distilled water and dried in a vacuum oven at 25 °C for 48 h.[17]

Preparation of bionanocomposite (LDH–MEF/GUM/CHIT). The preparation of LDH–MEF/GUM/CHIT was realized in several steps. In the first step, 1 g of GUM was added to 25 mL of distilled water and stirred (300 rpm) for 60 min at 70 °C.[18] Meanwhile, 0.2 g of LDH–Cl was placed in ultrasonic apparatus for 30 min and added to the solution of the first step. Simultaneously, 25 mL of MEF solution was also added to the above mixture and the pH of this mixture was raised to 10 by the addition of 0.2 mol L^{-1} NaOH solution. Then this

(CC) 2020 SCS.

mixture was maintained under magnetic stirring for 24 h. Afterward, the resulting solid was aged for 18 h, isolated by centrifugation, and washed with distilled water. Finally, the solid product was added to the homogeneous chitosan solution and subsequent steps were performed similarly to the preparation of LDH–MEF/CHIT.

The data related to drug adsorption and release are given as Supplementary material to this paper.

RESULTS AND DISCUSSION

XRD analysis

The XRD patterns of LDH–Cl, LDH–MEF, LDH–MEF/CHIT, and LDH MEF/GUM/CHIT are shown in Fig. 1. The XRD diffraction pattern of LDH–Cl was studied and the peaks (003), (006), (012), (015), (018), (110) confirmed the formation of the Mg–Al LDH structure.[19] LDH–Cl gives a distinct reflection peak at 2θ 11.45° with basal spacing 0.78 nm corresponding to (003) that indicates the initial LDH–Cl phase. LDH–MEF hybrid XRD patterns indicate the successful ion-exchange of chloride ions with MEF anions. The peak (003) of LDH–MEF is located at a lower angle (2θ 4.9) with a basal spacing of 1.82 nm, confirming intercalation of MEF anions in the intergallery space.

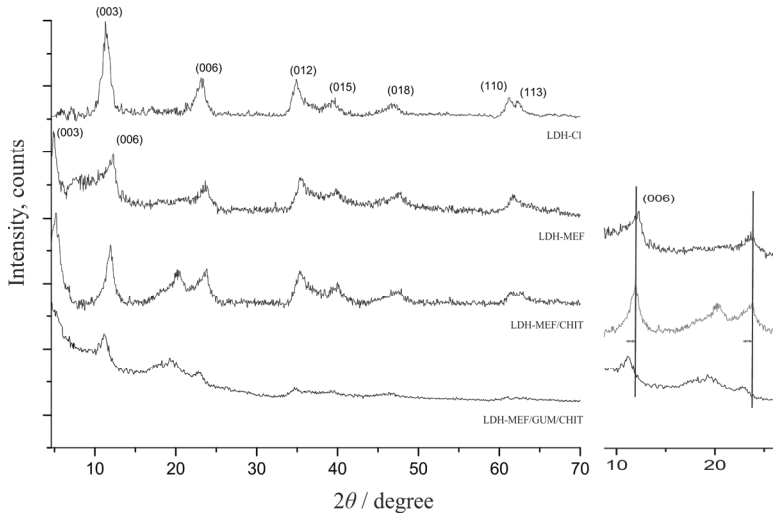

Fig. 1. XRD patterns of LDH–Cl, LDH–MEF, LDH–MEF/CHIT, and LDH MEF/GUM/CHIT.

Based on the basal spacing of 1.82 nm for LDH–MEF observed by XRD, and the thickness of the hydroxide layer of LDH (0.48 nm), the interlayer distance was calculated to be 1.34 nm. Due to the obtained value of interlayer distance and also considering the dimension of MEF molecule in Fig. S-1 of the Supplementary material to this paper (the length and width of MEF molecule were achieved employing Chemcraft software, 0.98 nm×0.90 nm), it could be expected the mefenamate anions arranged as a monolayer in the interlayer region

(CC) 2020 SCS.

of LDH. XRD analysis of pure chitosan shows a broad peak at 2θ 20°.[20] The LDH–MEF/CHIT and LDH–MEF/GUM/ /CHIT displayed weak peaks at around 2θ 20°, indicating chitosan coating on the surface of LDH.[21] When GUM and MEF are co-intercalated into the interlayer of LDH then small shifts in diffraction peaks to lower angles is seen for LDH–MEF/GUM/CHIT, and also the intensity of peaks and crystallinity of LDH are decreased with co-intercalating, confirming the co-intercalation of GUM/MEF into the interlayer of LDH.

FTIR spectroscopy

The FTIR spectra of the synthesized samples and MEF are shown in Fig. 2. The FTIR spectrum in Fig. 2B displays several characteristic bands of pure MEF, where the broad absorption bands at 3510 and 3311 cm^{-1} can be indexed to the stretching vibrations of O–H and N–H groups, respectively. The weak bands at 2965 and 2950 cm^{-1} are attributed to the asymmetric and symmetric vibrations of methyl group stretching, respectively. In addition, the peaks at 1592, 1577, 1507, 1470 and 1455 cm^{-1} are associated with stretching vibrations of the aromatic ring. Furthermore, two vibration bands at 1650 and 1326 cm^{-1} are ascribed to the asymmetric and symmetric stretching of carboxylate group, respectively. Finally, the wagging vibration of the N–H group is detected with a sharp peak at 876 cm^{-1}.[22]

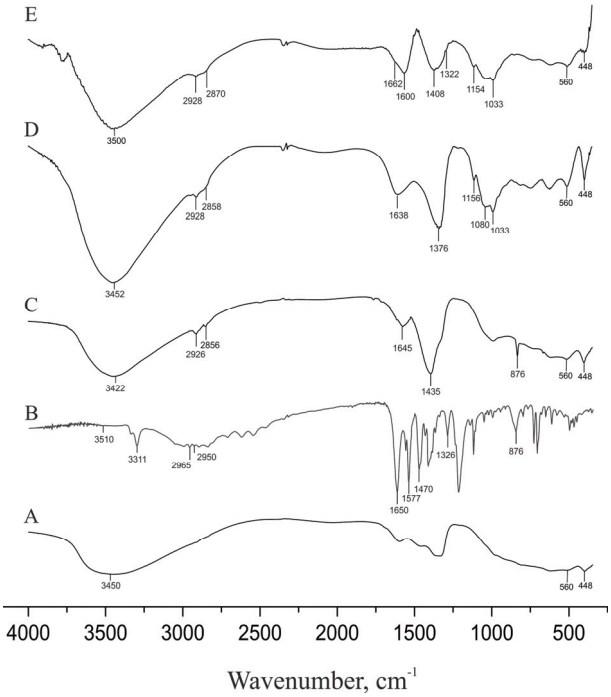

Fig. 2. FTIR spectra of LDH–Cl (A), MEF (B), LDH–MEF (C), LDH–MEF/CHIT (D) and LDH–MEF/GUM/CHIT (E).

(CC) 2020 SCS.

The FTIR spectrum of LDH–Cl is shown in Fig. 2A. As can be observed, the broad band at 3450 cm^{-1} originated from the hydroxyl group existing within the layer, while the bending vibration band at 1635 cm^{-1} corresponds to interlayer water molecules. Besides, the peaks at 560 and 448 cm^{-1} are assigned to the M–O (metal–oxygen) and M–O–M stretching vibrations in the inorganic layers of the LDH, respectively.[23]

The FTIR spectrum of the LDH–MEF is shown in Fig. 2C. The absorption bands at 1645 and 1435 cm^{-1} are related to the asymmetric and symmetric stretching vibrations of $-COO^-$. The peaks at 2928 and 2856 cm^{-1} represent asymmetric and symmetric stretching vibrations of the $-CH_3$ group. The broad absorbance peak at 3422 cm^{-1} is due to the –OH group and also water molecules that are physically adsorbed on the surface of LDH. The difference between wavenumber of the carboxylate stretching vibrations ($\Delta\nu = \nu_{as} - \nu_s$) can characterize the coordination sphere of carboxylate group. $\Delta\nu$ values <200 cm^{-1} indicate that the carboxylate group coordinates as a bidentate bridging ligand, whereas $\Delta\nu$ values >200 cm^{-1} represent carboxylate groups coordinate in the form of monodentate ligand.[24] In this work, the value of 210 cm^{-1} ($\Delta\nu$) for LDH–MEF demonstrates a monodentate coordination mode of the carboxylate group to metal (M^{II} or M^{III}) of the LDH lattice. Consequently, the FTIR spectrum of the LDH–MEF displayed several characteristic bands of MEF anions, confirming successful intercalation of MEF anions into the interlayers of LDH.

The FTIR spectrum in Fig. 2D demonstrates that surfaces of LDH–MEF/ /CHIT and LDH–MEF/GUM/CHIT are covered with chitosan. The band at 1156 cm^{-1} is due to the C–O stretching vibration. The alcohol vibration band is observed at 3452 cm^{-1}. The stretching band of aliphatic ether group is visible at 1080 cm^{-1}.[25] The peaks at 2928 and 2858 cm^{-1} indicate C–H asymmetric and symmetric stretch, which appeared more intense in comparison to those of LDH– –MEF.[26]

The FTIR spectrum of LDH–MEF/GUM/CHIT is shown in Fig. 2E, which also compares the spectra of the LDH–MEF/GUM/CHIT and LDH–MEF/CHIT. The vibration bands at 1662 and 1322 cm^{-1} verify the acetyl content of GUM. The predominant peaks at 1200–900 cm^{-1} are related to the content of carbohydrate content and glycosidic bond (C–O–C). In the spectra of LDH–MEF/GUM/ /CHIT, the peaks at 2928 and 2870 cm^{-1} are seen more strongly than LDH– –MEF/CHIT. This is due to the C–H vibrations of the GUM molecule.[27]

Thermal analysis

The TGA curves of MEF, CHIT, GUM, and synthesized samples are shown in Fig. 3. Fig. 3A shows the decomposition of MEF occurs in one step at 220 to 270 °C.[28] As is observed in Fig. 3A, CHIT displays two weight losses, the first between 25 and 140 °C, which are related to the vaporization of water adsorbed

(CC) 2020 SCS.

and the second of weight loss between 200 and 340 °C can be attributed to the degradation of CHIT.[29] The TGA curve of GUM in Fig. 3A displays a weight loss in two stages. The first stage ranges between 25–195 °C is due to the vaporization of surface moisture. The next weight loss stage between 200 and 335 °C relates to the degradation of the polysaccharide.[30]

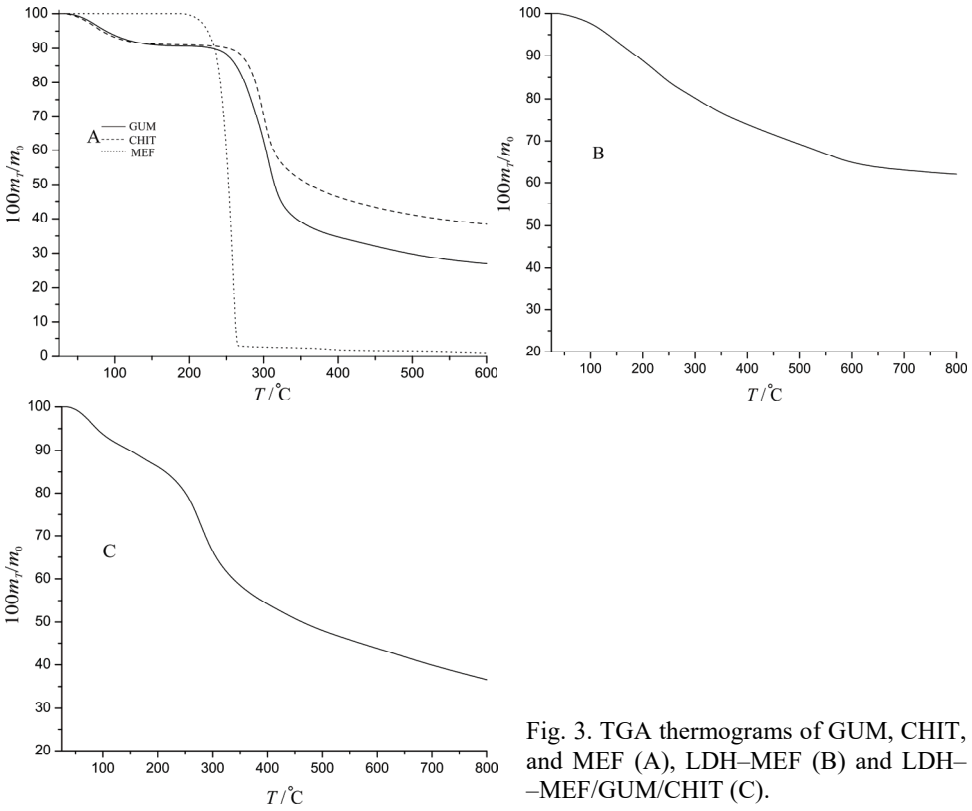

Fig. 3. TGA thermograms of GUM, CHIT, and MEF (A), LDH–MEF (B) and LDH––MEF/GUM/CHIT (C).

The TGA data of LDH–MEF (Fig. 3B) exhibited a weight loss from 25 °C (room temperature) up to 175 °C, which corresponds to the removal of physically surface adsorbed and interlayer water molecules. The LDH–MEF continues to lose weight from 175 to 415 °C, which indicates the decomposition of MEF and hydroxyl removal from the LDH layer.[22] Afterward, the weight loss that appeared above 450 °C corresponds to removal of chloride and combustion of MEF anions.[31] Based on the literature,[22] degradation of MEF intercalated into the LDH galleries occurred at 415 °C. This temperature is higher than the decay temperature of bare MEF (258 °C). This result indicates significant gain of thermal stability of intercalated MEF anion as compared to pure MEF.

(CC) 2020 SCS.

The weight loss of LDH–MEF/GUM/CHIT is shown in Fig. 3C, which exhibits a loss between 100–207 °C due to adsorbed water loss from the surface and the interlayer space. Heating at temperatures greater than 207 °C creates two weight loss events for LDH–MEF/GUM/CHIT. The weight loss between 207 and 355 °C is ascribed to the dehydroxylation from layer (LDH) and also to the main decomposition of the chitosan.[32] The second weight loss in the range 355–496 °C is attributed to combustion of the co-intercalated MEF/GUM.[30] The results obtained from thermal analysis indicate that the co-intercalation of MEF/GUM into the LDH leads to more thermal stability of the MEF as compared to LDH–MEF hybrid.

Morphology analysis

The FESEM images of CHIT, GUM, MEF, LDH–Cl, and LDH–MEF/GUM/CHIT were analyzed as depicted in Fig. 4. The FESEM of pure CHIT in Fig. 4A shows that it has a rugged surface with irregular morphology. Fig. 4B exhibits the morphology of individual GUM that also has a rugged surface and porous structure. Fig. 4C shows that the bare MEF particles are disordered in shape and vary remarkably in size.

The morphology of LDH–Cl (Fig. 4D, 1–2) displays a plate-like structure with a large range of particle sizes (14–23 nm). In Fig. 4E, 1–2, it is illustrated that after formation of LDH–MEF/GUM/CHIT, the plate-like structure was changed into a spherical shape, and the particle size was increased (32–42 nm) in comparison with LDH–Cl. Therefore, the results show that the co-intercalation of MEF/GUM into the LDH interlayer resulted in surface morphology converting from a uniform plate-like shape with nanosheet structure to disordered granular structure. Figs. 4F and G show the EDS spectra of LDH–Cl and LDH–MEF/GUM/CHIT. The EDS analysis of LDH–Cl clearly revealed that peaks of Mg, Al, O and Cl were present. Fig. 4G shows the EDS of LDH–MEF/GUM/CHIT that confirms the presence of Mg, Al, O, C and N as the main elements of the bionanocomposite. Furthermore, the decrease in the peak of Cl in the EDS spectrum of the bionanocomposite (Fig. 4G) confirms that the Cl ions were replaced with MEF anions.[33]

Release study

In this study, the release of MEF from LDH–MEF, LDH–MEF/CHIT, and LDH MEF/GUM/CHIT were investigated in simulated gastric fluid (pH 1.2) and simulated intestinal fluid (pH 7.4) at 37 °C. The graph of Fig. 5A shows LDH–MEF released 58 % of MEF in 60 min, while in the same time, LDH–MEF/CHIT and LDH–MEF/GUM/CHIT released about 48 and 34 % of MEF into the simulated gastric environment, respectively. Therefore, the release rate of MEF from LDH–MEF/CHIT and LDH–MEF/GUM/CHIT was slower than that from

(CC) 2020 SCS.

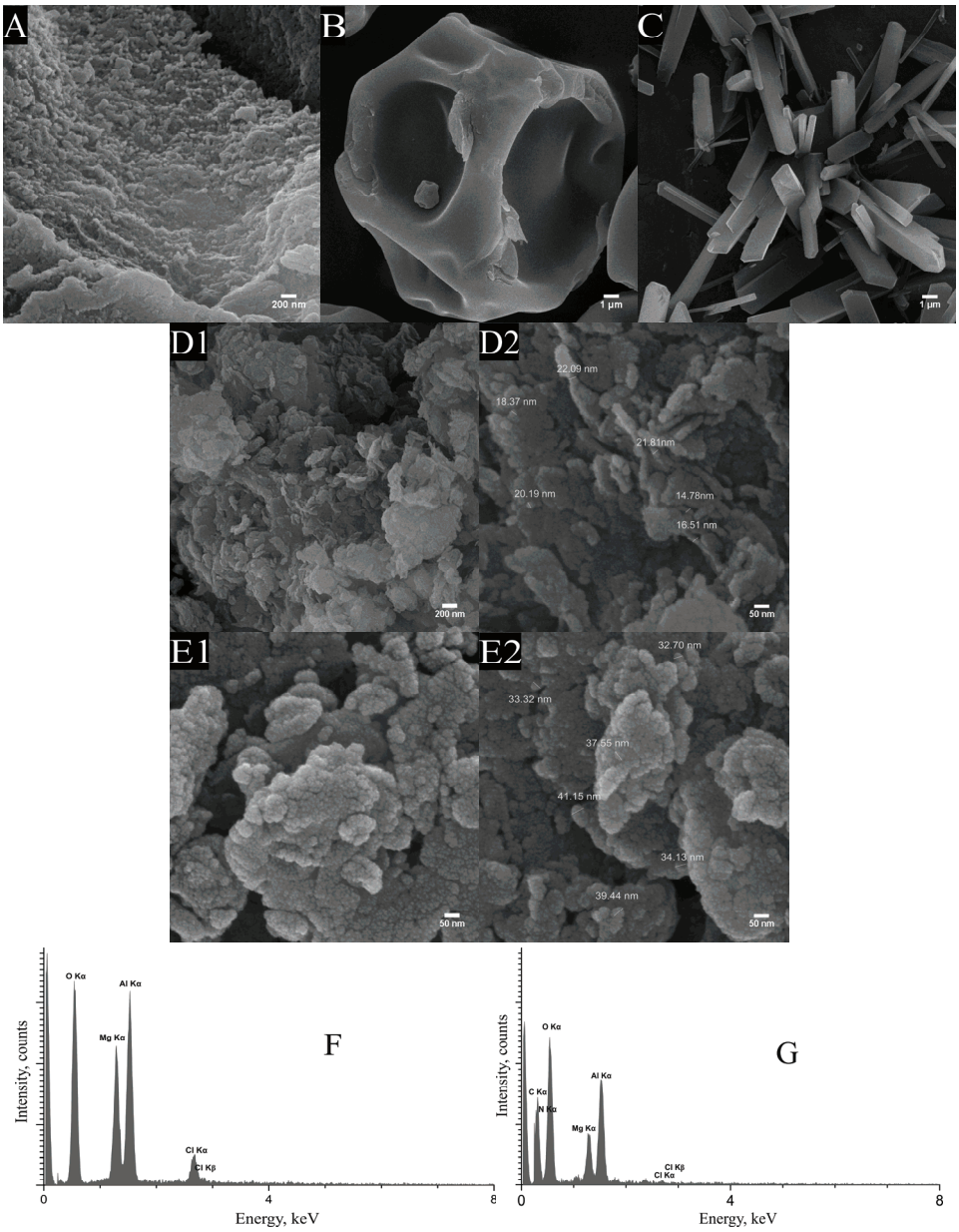

Fig. 4. FESEM image of CHIT (A), GUM (B), MEF (C), LDH–Cl (D1–2), LDH–MEF/ /GUM/CHIT (E1–2), and EDS spectra of LDH–Cl (F) and LDH–MEF/GUM/CHIT (G).

LDH–MEF, which is due to the chitosan coating on the surface of the LDH that prevent MEF release. Actually, in acidic pH, the $–NH_2$ group in the structure of chitosan changes to $–NH_3^+$ and decreases the penetration of water molecules into

(CC) 2020 SCS.

the bionanocomposite.[34] In addition, the existence of gum arabic in LDH–MEF/ /GUM/CHIT is a second barrier for MEF release. In an acidic environment (pH 1.2), the LDH framework may easily be dissolved and the intercalated MEF rapidly released, but due to the presence of gum arabic between the LDH layers as a hydrochloric acid inhibitor, the resistance of the LDH gallery increases.[35] The release profiles of MEF from the three carriers in phosphate buffer (pH 7.4) are presented in Fig. 5B. As is shown, MEF was released with a gentle slope from the three carriers. This slow release is related to strong electrostatic interactions between the MEF anions and the positively charged LDH layers. LDH–MEF, LDH–MEF/CHIT, and LDH–MEF/GUM/CHIT released approximately 53, 37, and 12 % of MEF in 180 min, respectively. This apparent difference in MEF release is related to the stability of the structure of LDH–MEF/GUM/CHIT in phosphate buffer. When LDH–MEF/GUM/CHIT disperses into a phosphate buffer solution, the negative charge density of GUM increases between the layers of LDH, which lead to greater electrostatic attraction with positively charge layers of LDH.[36] This results in increased stability of LDH–MEF/GUM/CHIT in the phosphate buffer. Thus, MEF is released at a slower rate in comparison with its release from LDH–MEF and LDH–MEF/CHIT.

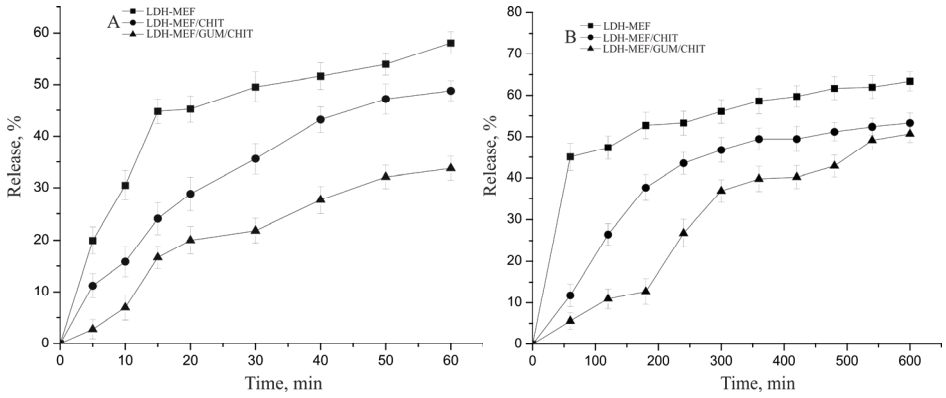

Fig. 5. The release profiles of MEF from LDH–MEF, LDH–MEF/CHIT, and LDH–MEF/GUM/CHIT in simulated gastric fluid at pH=1.2 for 60 min (A) and a simulated intestinal fluid at pH 7.4 for 600 min (B) at 37 °C.

CONCLUSIONS

In this research, MEF/GUM was successfully co-intercalated into the interlayer spaces of LDH and then the surface of LDH was covered with chitosan. The advantages of the presented method for preparing the bionanocomposite are that it does not require toxic organic solvents, a high-temperature, or long times. The interaction between the layers of LDH and GUM with different charges could produce a strong organic–inorganic matrix that resulted in the slow release

(CC) 2020 SCS.

of the intercalated MEF anions in phosphate buffer. The loading percentage of MEF in the bionanocomposite was estimated to be about 44 %. In other experiments, three adsorption isotherms were investigated in the interaction of MEF with LDH–Cl, and the results showed that the Langmuir adsorption isotherm was consistent. The adsorption of MEF into the layers of LDH was found to follow pseudo-second-order kinetics (R^2 = 0.999). The obtained results confirmed that the bionanocomposite has better thermal stability than that of the free drug, LDH–MEF, LDH–MEF/CHIT. The MEF release from all LDH samples was seen to follow the Korsmeyer–Peppas pattern and non-Fickian transport process. In conclusion, the bionanocomposite was highly capable of sustained release of anti-inflammatory drugs.

Acknowledgements. The authors wish to thank the Islamic Azad University of Varamin-Pishva for the support of this research.

SUPPLEMENTARY MATERIAL

Additional data are available electronically at the pages of journal website: https://www.shd-pub.org.rs/index.php/JSCS/index, or from the corresponding author on request.

ИЗВОД

ДОБИЈАЊЕ БИОНАНОКОМПОЗИТА НА БАЗИ LDH КОРИШЋЕЊЕМ БИОПОЛИМЕРА ГУМАРАБИКЕ И ПРЕВЛАКЕ ОД ЦИТОЗАНА ЗА КОНТРОЛИСАНО ОТПУШТАЊЕ ЛЕКА

MILAD ABNIKI, ALI MOGHIMI и FARIBORZ AZIZINEJAD

Department of Chemistry, Varamin-Pishva Branch, Islamic Azad University, Varamin, Iran

У овом раду је предложена нова формулација за контолисано отпуштање анјона мефенаминске киселине (MEF) интеркалираног у Mg–Al слојевити двоструки хидроксид (LDH) за оралну примену. Испитиван је утицај различитих експерименталних услова на инкорпорирање МЕФ и гумарабике (GUM) у LDH структуру. На добијене LDH–MEF и LDH–MEF/GUM нанет је цитозан (CHIT). Додатно, LDH–Cl је коришћен за адсорпцију анјона MEF и испитивање механизма. За карактеризацију синтетисаних узорака на бази LDH коришћене су различите технике: FESEM (скенирајућа електронска микроскопија), XRD (рендгенска дифракциона анализа), FTIR (инфрацрвена спектроскопија) и TGA (термогравиметријска анализа). XRD и FTIR анализе су потврдиле да су MEF и GUM ефикасно интеркалирани у међуслојни простор LDH. TG анализа је показала да је повећана термичка стабилност интеркалираног MEF у облику бионанокомпозита (LDH–MEF/GUM/CHIT). Коначно, in vitro експерименти отпуштања из бионанокомпозита при pH 1,2 (кисела средина) и pH 7,4 (фосфатни пуфер) су показали контролисано отпуштање анјона мефенаминске киселине као модела лека против упалних процеса.

(Примљено11. октобра, ревидирано 12. децембра 2019, прихваћено 14. јануара 2020)

REFERENCES

1. C. S. Ha, J. A. Gardella, Jr., *Chem. Rev.* **105** (2005) 4205 (http://dx.doi.org/10.1021/cr040419y)
2. R. Omidirad, F. H. Rajabi, B. V. Farahani, *J. Serb. Chem. Soc.* **78** (2013) 1609 (http://dx.doi.org/10.2298/jsc121225041o)

(CC) 2020 SCS.

3. T. N. Rao, P. Babji, N. Ahmad, R. A. Khan, I. Hassan, S. A. Shahzad, F. M. Husain, *Saudi J. Biol. Sci.* (2019) (http://dx.doi.org/10.1016/j.sjbs.2019.09.005)
4. P. Colombo, R. Bettini, P. Santi, A. De Ascentiis, N. Peppas, *J. Control. Release* **39** (1996) 231 (http://dx.doi.org/10.1016/0168-3659(95)00158-1)
5. H. Merine, H. Merine, *Indian J. Pharm. Educ.* **49** (2015) 301 (http://dx.doi.org/10.5530/ijper.49.4s.6)
6. S. S. Ray, M. Okamoto, *Prog. Polym. Sci.* **28** (2003) 1539 (http://dx.doi.org/j.progpolymsci.2003.08.002)
7. M. Alexandre, P. Dubois, *Mater. Sci. Eng., R* **28** (2000) 1 (http://dx.doi.org/10.1016/s0927-796x(00)00012-7)
8. A. K. Kodoth, V. M. Ghate, S. A. Lewis, B. Prakash, V. Badalamoole, *Int. J. Biol. Macromol.* **134** (2019) 269 (http://dx.doi.org/10.1016/j.ijbiomac.2019.04.191)
9. A. Kurowska, V. Ghate, A. Kodoth, A. Shah, A. Shah, B. Vishalakshi, B. Prakash, S. A. Lewis, *Pharm. Res.* **36** (2019) 122 (http://dx.doi.org/10.1007/s11095-019-2658-8)
10. E. Ruiz-Hitzky, M. Darder, P. Aranda, K. Ariga, *Adv. Mater.* **22** (2010) 323 (http://dx.doi.org/10.1002/adma.200901134)
11. F. Cavani, F. Trifiro, A. Vaccari, *Catal. Today* **11** (1991) 173 (http://dx.doi.org/10.1016/0920-5861(91)80068-k)
12. M. Silion, D. Hritcu, I. M. Jaba, B. Tamba, D. Ionescu, O. C. Mungiu, I. M. Popa, *J. Mater. Sci.: Mater. Med.* **21** (2010) 3009 (http://dx.doi.org/10.1007/s10856-010-4151-0)
13. T. Xu, J. Zhang, H. Chi, F. Cao, *Acta Biomater.* **36** (2016) 152 (http://dx.doi.org/10.1016/j.actbio.2016.02.041)
14. Q. Zhai, H. Li, Y. Song, R. Wu, C. Tang, X. Ma, Z. Liu, J. Peng, J. Zhang, Z. Tang, *AAPS PharmSciTech* **19** (2018) 2048 (http://dx.doi.org/10.1208/s12249-018-1011-6)
15. R. Chitrakar, S. Tezuka, A. Sonoda, K. Sakane, T. Hirotsu, *Ind. Eng. Chem. Res.* **47** (2008) 4905 (http://dx.doi.org/10.1021/ie0716417)
16. V. R. Cunha, V. A. Guilherme, E. De Paula, D. R. De Araujo, R. O. Silva, J. V. Medeiros, J. R. Leite, P. A. Petersen, M. Foldvari, H. M. Petrilli, V. R. Constantino, *Mater. Sci. Eng., C* **58** (2016) 629 (http://dx.doi.org/10.1016/j.msec.2015.08.037)
17. C. M. Futalan, Y.-S. Huang, J.-H. Chen, M.-W. Wan, *Water Sci. Technol.* **78** (2018) 676 (http://dx.doi.org/10.2166/wst.2018.339)
18. S. Iftekhar, V. Srivastava, D. L. Ramasamy, W. A. Naseer, M. Sillanpää, *Chem. Eng. J.* **347** (2018) 398 (http://dx.doi.org/10.1016/j.cej.2018.04.126)
19. S. Miyata, *Clays Clay Miner.* **23** (1975) 369 (http://dx.doi.org/10.1346/ccmn.1975.0230508)
20. S. Kumar, J. Koh, *Int. J. Mol. Sci.* **13** (2012) 6102
21. M. Nikkhoo, M. Amini, S. M. F. Farnia, G. R. Mahdavinia, S. Gautam, K. H. Chae, *J. Inorg. Organomet. Polym. Mater.* (2018) 1 (http://dx.doi.org/10.1007/s10904-018-0861-4)
22. M. Del Arco, A. Fernández, C. Martín, V. Rives, *Appl. Clay Sci.* **36** (2007) 133 (http://dx.doi.org/10.1016/j.clay.2006.04.011)
23. S. Senapati, R. Thakur, S. P. Verma, S. Duggal, D. P. Mishra, P. Das, T. Shripathi, M. Kumar, D. Rana, P. Maiti, *J. Control. Release* **224** (2016) 186 (http://dx.doi.org/10.1016/j.jconrel.2016.01.016)
24. C. Li, G. Wang, D. G. Evans, X. Duan, *J. Solid State Chem.* **177** (2004) 4569 (http://dx.doi.org/10.1016/j.jssc.2004.09.005)
25. A. Moghimi, *Russ. J. Phys. Chem., A* **88** (2014) 2157 (http://dx.doi.org/10.1134/S0036024414120024)

(CC) 2020 SCS.

26. A. Moghimi, *Russ. J. Phys. Chem., A* **87** (2013) 1203 (http://dx.doi.org/10.1134/s0036024413070388)
27. P. Barik, A. Bhattacharjee, M. Roy, *Bull. Mater. Sci.* **38** (2015) 1609 (http://dx.doi.org/10.1007/s12034-015-0961-5)
28. T. Hładoń, J. Pawlaczyk, B. Szafran, *J. Inclusion Phenom. Macrocyclic Chem.* **35** (1999) 497 (http://dx.doi.org/10.1023/A:1008048612736)
29. N. G. Kandile, H. M. Mohamed, *Int. J. Biol. Macromol.* **122** (2019) 578 (http://dx.doi.org/10.1016/j.ijbiomac.2018.10.198)
30. C. Cozic, L. Picton, M.-R. Garda, F. Marlhoux, D. Le Cerf, *Food Hydrocoll.* **23** (2009) 1930 (http://dx.doi.org/10.1016/j.foodhyd.2009.02.009)
31. W. Meng, F. Li, D. G. Evans, X. Duan, *Mater. Res. Bull.* **39** (2004) 1185 (http://dx.doi.org/10.1016/j.materresbull.2004.04.016)
32. C. Tang, T. Zhou, J. Yang, Q. Zhang, F. Chen, Q. Fu, L. Yang, *Colloids Surfaces, B Biointerfaces* **86** (2011) 189 (http://dx.doi.org/10.1016/j.colsurfb.2011.03.041)
33. J. Chen, Y. Du, W. Que, Y. Xing, X. Chen, B. Lei, *Colloids Surfaces, B* **136** (2015) 126 (http://dx.doi.org/10.1016/j.colsurfb.2015.08.053)
34. S. M. Ahsan, M. Thomas, K. K. Reddy, S. G. Sooraparaju, A. Asthana, I. Bhatnagar, *Int. J. Biol. Macromol.* **110** (2018) 97 (http://dx.doi.org/10.1016/j.ijbiomac.2017.08.140)
35. K. Azzaoui, E. Mejdoubi, S. Jodeh, A. Lamhamdi, E. Rodriguez-Castellón, M. Algarra, A. Zarrouk, A. Errich, R. Salghi, H. Lgaz, *Corros. Sci.* **129** (2017) 70 (http://dx.doi.org/10.1016/j.corsci.2017.09.027)
36. L. Bai, F. Liu, X. Xu, S. Huan, J. Gu, D. J. Mcclements, *J. Food Eng.* **207** (2017) 35 (http://dx.doi.org/10.1016/j.jfoodeng.2017.03.021).

(CC) 2020 SCS.